Inorganica Chimica Acta, 141 (1988) 185–192

On the Nature of the High-spin ($^6A_1$) ⇌ Low-spin ($^2T_2$) Transition in [Fe(3-$CH_3OSPH)_2$]Y Complexes

MADAN MOHAN, NIRANJAN S. GUPTA, LAKHAMI CHANDRA
Department of Chemistry, N.R.E.C. College, Khurja-203 131 (U.P.), India
NARENDRA K. JHA
Department of Chemistry, Indian Institute of Technology, Hauz Khas, New Delhi-110 016, India
and RADHEY S. PRASAD
Department of Chemistry, St. Columba's College, Hazari Bag-825 301, Bihar, India

(Received March 31, 1987)

Abstract

The spin-crossover phenomenon between the low-spin ($S = 1/2$, $^2T_2$) and high-spin ($S = 5/2$, $^6A_1$) states depending on temperature is examined for two complexes of the composition [Fe(3-$CH_3OSPH)_2$]Y, where 3-CH_3OSPH is the monoanionic Schiff base N_2O ligand derived from the condensation of 3-methoxysalicylaldehyde and 2-pyridylhydrazine, and Y is either PF_6^- or BPh_4^-. Variable temperature magnetic susceptibility, EPR, Mössbauer, and electronic data are analysed for these two complexes. Both are seen to undergo gradual but complete spin-crossover transformation from high-spin to low-spin in the solid state. The relaxation time of the change from the high-spin to the low-spin state (and vice versa) in [Fe(3-$CH_3OSPH)_2$]PF_6 is slower than the ^{57}Fe Mössbauer time scale, while [Fe(3-$CH_3OSPH)_2$]-BPh_4 shows a single quadrupole-split doublet in the Mössbauer spectrum from 80 to 298 K. The results are interpreted in terms of a model in which the spin-interchange crossing is treated as an intramolecular mechanism, internal electron-transfer reaction. EPR spectra show that the [Fe(3-$CH_3OSPH)_2$]$^+$ series has one unpaired electron in a d_{xy} orbital.

Introduction

Recently, much interest has been shown in the solid-state spin-crossover transformations which provide a means for investigating just how an intramolecular (the high-spin ⇌ low-spin interconversion) is coupled to the intermolecular interactions inherent to the solid state. In the ferric ion, the spin-crossover event involves an intramolecular transfer of two electrons in the t_{2g} and e_g orbitals. Recent research in the area [1–4] of spin-crossover chemistry has focused to a greater extent on understanding the factors that affect the thermodynamics at the spin-crossover transformation and to a lesser extent on the means by which intermolecular interactions inhibit or enhance the rates of intramolecular spin-state interconversions.

The spin-state interconversion rates for spin-crossover solids have typically been estimated relative to the time scales associated with various spectroscopic techniques (for Mössbauer $\tau \sim 10^7$ s^{-1} and for EPR $\tau \sim 10^{10}$ s^{-1}). Previously, only the ferric dithiocarbamates [5], monothiocarbamates [6] and diselenocarbamates [7] were known to interconvert rapidly relative to the Mössbauer time scale. Maeda *et al.* [8–11] and Hendrickson *et al.* [12–15] have recently reported a number of new iron(III) complexes with N_4O_2 and N_6O_2 ligand donor systems which undergo rapid spin-state interconversion on the Mössbauer time scale and slow interconversion on the EPR time scale. The spin-state interconversion rates in these FeN_4O_2 and FeN_6O_2 systems appear to be extremely sensitive to small molecular and structural changes. Maeda *et al.* [11] have established that counter ion and ligand substituent changes can dramatically alter the nature of the Mössbauer spectra. However, the exact origins of these effects are unknown.

In the light of Maeda's report [11] of the sensitivity of the spin-state interconversion rates to the counterion and ligand substituent changes, we report, in this paper, the results of spectroscopic and magnetic investigations of [Fe(3-$CH_3OSPH)_2$]Y complexes.

Experimental

Preparation of Compounds

All elemental analyses were carried out at the Microanalytical Laboratory of Central Drug Research

0020-1693/88/$3.50

Institute (C.D.R.I.), Lucknow-226 001. (U.P.). The ligands used in this study were the Schiff base condensation products of 2-pyridylhydrazine with 3-methoxysalicylaldehyde which were obtained as commercially available products from Aldrich Chemical Co. The ligand obtained is abbreviated as 3-CH_3OSPH.

[Fe(3-CH_3OSPH)$_2$]Cl

The Schiff base ligand (3-CH_3OSPH) was prepared by adding a solution of 2-pyridylhydrazine (1.09 g, 10 mmol) in 20 ml of methanol to a solution of 3-methoxysalicylaldehyde (1.52 g, 10 mmol) in 20 ml of methanol. The solution mixture was heated on a steam bath until it turned yellow. Sodium hydroxide (0.4 g) dissolved in 10 ml of H_2O was then added to this solution and was stirred for a further 15 min. To this solution was slowly added $FeCl_3$ (0.81 g, 5 mmol) in 15 ml of methanol. Addition of the ferric salt solution led to the immediate precipitation of black microcrystals, which were isolated by filtration, washed with methanol and ether, and then dried *in vacuo* over P_2O_5 to give 90% of the product. *Anal.* Calc. for $FeC_{26}H_{24}N_6O_4Cl$: C, 54.23; H, 4.17; N, 14.60; Fe, 9.69. Found: C, 53.80; H, 4.42; N, 14.55; Fe, 9.80%.

[Fe(3-CH_3OSPH)$_2$]NO_3

The yellow Schiff base solution was formed by heating on a steam bath a solution of 3-methoxysalicylaldehyde (1.52 g, 10 mmol) in 20 ml of methanol with a solution of 2-pyridylhydrazine (1.09 g, 10 mmol) in 20 ml of methanol for 20 min. Sodium hydroxide (0.4 g) dissolved in 10 ml of H_2O was added to the solution and stirred for an additional 15 min. To this solution was slowly added $Fe(NO_3)_3 \cdot 9H_2O$ (2.0 g, 5 mmol) dissolved in 15 ml of methanol, producing a colour change from yellow to blue–violet. After overnight refrigeration, the reaction mixture afforded black microcrystals, which were isolated by filtration, washed with methanol and ether, and dried *in vacuo* over P_2O_5 to give 90% of the product. *Anal.* Calc. for $FeC_{26}H_{24}N_6O_7$: C, 51.84; H, 3.98; N, 16.28; Fe, 9.27. Found: C, 51.21; H, 4.12; N, 16.31, Fe, 9.40%.

[Fe(3-CH_3OSPH)$_2$]PF_6

The yellow Schiff base solution, consisting of 3-methoxysalicylaldehyde (1.52 g, 10 mmol) and 2-pyridylhydrazine (1.09 g, 10 mmol) in 25 ml of methanol, was prepared as above and combined with 10 ml of a methanolic solution of NH_4PF_6 (1.6 g, 10 mmol). To the resulting mixture was introduced a solution of $Fe(NO_3)_3 \cdot 9H_2O$ (2.0 g, 5 mmol) in 15 ml of methanol as several small aliquots with constant stirring. The dark purple microcrystals that formed within a minute were isolated by filtration, washed with methanol and ether, and dried over P_2O_5 *in vacuo* to give 72% of the product. *Anal.* Calc. for $FeC_{26}H_{24}N_6O_4PF_6$: C, 45.56; H, 3.50; N, 12.26; Fe, 8.15. Found: C, 45.02; H, 3.72; N, 12.02; Fe, 8.21%.

[Fe(3-CH_3OSPH)$_2$]BPh_4

This product was prepared by the metathesis of the NO_3^- salt with $NaBPh_4$ in methanol. The dark purple microcrystalline solid was dried *in vacuo* over P_2O_5. *Anal.* Calc. for $FeC_{50}H_{44}N_6O_4B$: C, 69.88; H, 5.12; N, 9.78; Fe, 6.49. Found: C, 69.34; H, 5.37; N, 9.42; Fe, 6.58%.

Magnetic Susceptibilities

Variable temperature magnetic susceptibilities were determined on a vibrating-sample magnetometer. The magnetometer was calibrated with $CuSO_4 \cdot 5H_2O$, and a calibrated Ga As diode was used for sample temperature determination and control. For all data diamagnetic corrections, estimated from Pascal's constants [16], were used in the calculation of molar paramagnetic susceptibilities.

EPR Spectra

Electron paramagnetic resonance data (x-band) were obtained on a Varian E-4 spectrometer, using DPPH as a reference material. Variable temperatures (300–130 K) were obtained with the use of a gas-flow cavity insert and a Varian V-4540 temperature controller. Temperatures were determined before and after each spectrum with a copper–constantan thermocouple, and the temperature accuracy was estimated to be ±5 K. A direct immersion dewar, which was inserted into the cavity, was used to obtain spectral data at 78 K.

Mössbauer Spectra

Mössbauer spectral data were collected on polycrystalline samples by using a constant-acceleration spectrometer which was calibrated with natural α-iron foil. The source was $^{57}Co(Cu)$ and was maintained at room temperature for all experiments. A copper–constantan thermocouple, mounted on the sample-cell holder, was used to monitor the sample temperature. The absolute precision is estimated to be ±3 K. A computer program was used to fit the Mössbauer absorptions to Lorentzian line shapes.

Electronic Spectra

The electronic absorption spectra of the methanolic solution containing the samples (3×10^{-3} mol/l) were recorded on Unicam SP 700 spectrophotometer.

Conductance Measurements

The solution conductivities of the samples in methanol (1×10^{-3} mol/l) at 25 °C were measured on a Toshniwal conductivity bridge type CL 01/01.

Results and Discussion

The pseudooctahedral iron(III) complexes with an N_4O_2 coordination core were prepared, using as a ligand the Schiff base condensation product of 3-methoxysalicylaldehyde with 2-pyridylhydrazine. The ligand is deprotonated to afford a monoanionic tridentate N_2O ligand. The overall reaction is:

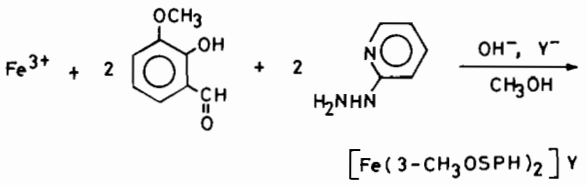

where Y is Cl^-, NO_3^-, PF_6^- or BPh_4^-. The monoanionic ligand is:

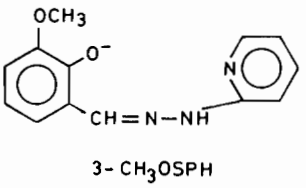

3-CH_3OSPH

All the complexes are quite stable at room temperature and do not show any sign of decomposition after a long period of standing. All the complexes are soluble in a number of solvents of moderate-to-good coordinating ability, such as dimethylformamide, dimethylsulphoxide, methanol, ethanol, and pyridine. The molar conductance of the complexes in methanol at $\sim 10^{-3}$ M lie in the 110–117 ohm^{-1} cm^2 mol^{-1} range, indicating their uni-univalent electrolytic behaviour in solution.

In the absence of a single-crystal X-ray study, it is difficult to suggest whether the tridentate 3-CH_3OSPH ligand is arranged around the iron(III) ion in a facial or meridional configuration. The iron(III) cations present in these complexes are meridional, as pictured in Fig. 1, may be inferred from several pieces of indirect evidence. An X-ray structural study has been reported for several analogues of these iron(III) complexes, where two tridentate Schiff base ligands with ethylene linkages between imine and amine nitrogen donors are present [17–19]. Structural data are also available [20] for ferric complexes with hexadentate N_4O_2 ligands derived from triethylenetetramine. The single-crystal X-ray study of these analogues has invariably shown that the geometry is meridional, where the oxygen atoms on the two ligands are located *cis* relative to each other and the imino nitrogen atoms are *trans*.

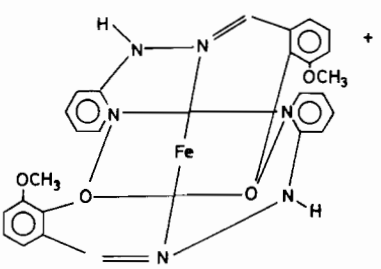

Fig. 1. Proposed meridional (*cis* oxygen) structure for the iron(III) complexes.

Magnetic Susceptibility

Variable temperature magnetic susceptibility data in the 78–300 K range for [Fe(3-$CH_3OSPH)_2$]Y are illustrated in Fig. 2. As is evident in Fig. 2, the compounds show gradual and nearly complete spin-crossover transformations. For compound [Fe(3-$CH_3OSPH)_2$]BPh_4 the transformation is nearly complete, whereas the compound [Fe(3-$CH_3OSPH)_2$]PF_6 shows appreciable low-spin population (~45%) at room temperature. It appears that the high-spin molecules in [Fe(3-$CH_3OSPH)_2$]BPh_4 are favoured due to the lattice expansions resulting from the large BPh_4 counterion [15].

Assuming μ_{eff} (high-spin) = 5.99 μ_B and μ_{eff} (low-spin) = 1.90 μ_B, the high- and low-spin population factions can be estimated and converted into equilibrium constant data (K_{eq}), where K_{eq} = (fraction of high-spin)/(1 − fraction high-spin). The changes of the enthalpy (ΔH) and entropy (ΔS) for spin-crossover 'reactions' can be calculated from plots of ln K_{eq} *versus* reciprocal temperature. The compounds

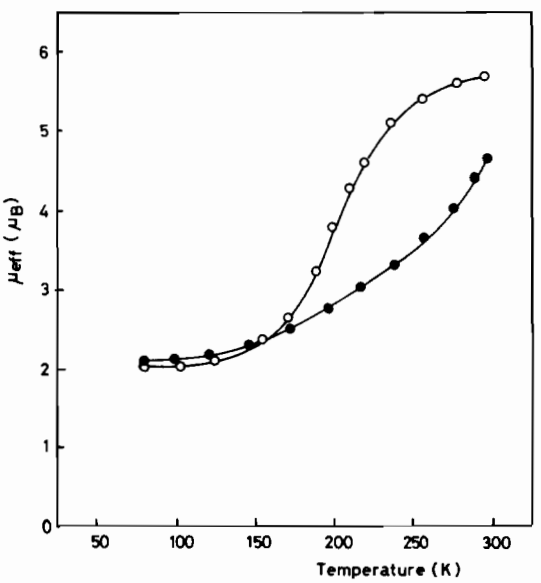

Fig. 2. Effective magnetic moments *vs.* temperature plots for [Fe(3-$CH_3OSPH)_2$]PF_6 (I) (•) and [Fe(3-$CH_3OSPH)_2$]BPh_4 (II) (○). Solid lines are drawn for clarity only and do not show data fittings or simulations.

yield nonlinear $\ln K_{eq}$ *versus* $1/T$ curves, which should not be considered as evidence for cooperativity in the spin-crossover transformation; solid-state transformations can exhibit nonlinear $\ln K_{eq}$ *versus* $1/T$ behaviour for a variety of circumstances [21]. The remaining compounds are essentially low-spin complexes. It appears that in the $[Fe(3\text{-}CH_3OSPH)_2]Y$ series the Cl^- and NO_3^- counterions tend to give low-spin complexes, and the BPh_4^- and PF_6^- counterions give complexes which show spin-crossover phenomenon. Such magnetic behaviour, depending on the nature of the counterion, has already been observed for the ferric X-SalEen [22], X-Salmeen [23] and 3-OEt-SalBzen [19] complexes.

Mössbauer Spectroscopy

Variable temperature Mössbauer spectral data for $[Fe(3\text{-}CH_3OSPH)_2]PF_6$ complex are illustrated in Fig. 3. The spectra between 80 and 165 K are characterized by the quadrupole splitting $\Delta E_Q = 2.874$–2.834 mm/s, the values being typical for a low-spin ^2T ground state of iron(III). At 190 K, a second weak doublet is clearly recognized, its intensity increases with increasing temperature, while that of first doublet is simultaneously decreasing, *cf.* spectrum at 240 K. At 260 K, the contribution of the second doublet is clearly predominant, and at 300 K, it is almost the only one present. On the basis of the Mössbauer parameters, *i.e.* $\Delta E_Q = 1.02$ mm/s, $\delta = 0.342$ mm/s at 300 K, the second doublet is assigned to the high-spin ^6A ground state of iron(III). It is thus evident that a low-spin $\rightleftharpoons$ high-spin transition is involved in the $[Fe(3\text{-}CH_3OSPH)_2]PF_6$ complex. The temperature dependence of the area fraction of a high-spin species $S(HS)$ *versus* the total absorption area is illustrated in Fig. 4. The curve is consistent with that of the population probability of the high-spin fraction calculated from the μ_{eff} values on the assumption that μ_{eff} (high-spin) = 5.99 μ_B and μ_{eff} (low-spin) = 1.90 μ_B. The temperature dependence of the recoil-free fractions is given by the temperature dependence of the area under the resonance curve. The Debye model approximation leads [24] to $d \ln f/dT \propto d \ln A/dT$ in the high temperature limit. The plots of $\ln[A(T)/A(81)]$ *versus* T for $[Fe(3\text{-}CH_3OSPH)_2]PF_6$ complex (Fig. 4) show a discontinuity in the temperature range between 165–190 K, indicating that some kind of phase transition occurs in this temperature range, if spin transition accompanies the intermolecular or lattice vibrational change. The appearance of two pairs of a doublet in the Mössbauer spectra means that the rate of the spin-crossover between the low- and high-spin states is slow relative to the life time of the excited Mössbauer nuclear state ($\tau \simeq 10^7$ s^{-1}).

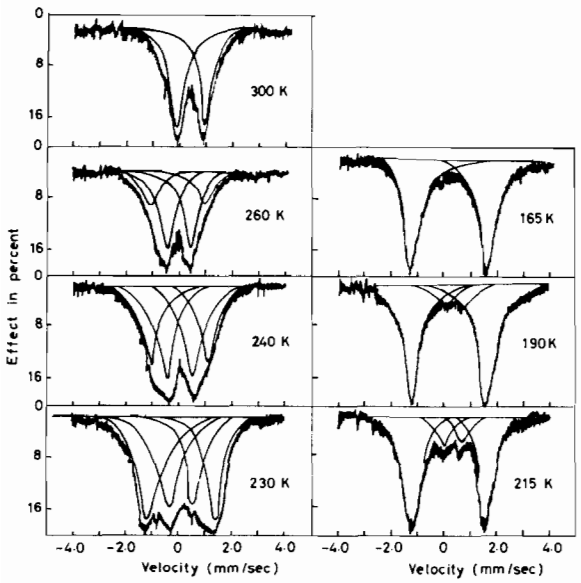

Fig. 3. ^{57}Fe Mössbauer spectra of $[Fe(3\text{-}CH_3OSPH)_2]PF_6$ at various temperatures.

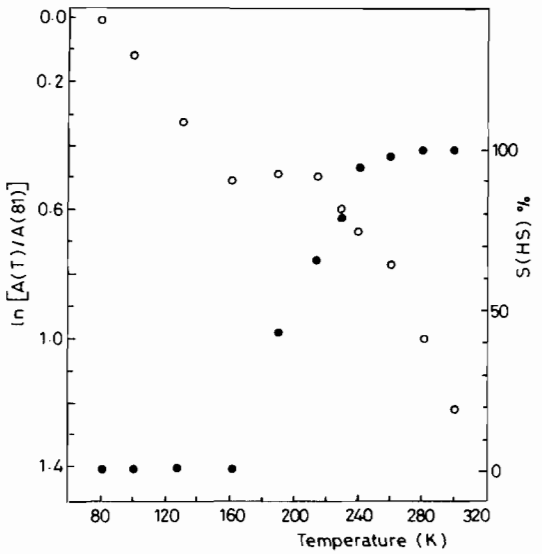

Fig. 4. Temperature dependence of the $\ln[A(T)/A(81)]$ (○) and $S(HS)\%$ (●) for the $[Fe(3\text{-}CH_3OSPH)_2]PF_6$ complex.

Variable temperature Mössbauer spectra of the $[Fe(3\text{-}CH_3OSPH)_2]BPh_4$ complex are illustrated in Fig. 5. The spectra between 80 and 165 K are typical for the low-spin iron(III) complexes and are characterized by $\Delta E_Q = 2.384$–2.352 mm/s and $\delta = 0.237$–0.326 mm/s. The spectrum at 298 K is characterized by a broad asymmetric doublet with $\Delta E_Q = 0.892$ mm/s and $\delta = 0.398$ mm/s ascribed to a high-spin iron(III) state. A single quadrupole-split doublet with a broad linewidth is observed in the temperature range of 165–298 K. This indicates that the relaxation time to change from low-spin state to high-spin state and vice versa is shorter than the lifetime of the excited Mössbauer nuclear state and that the nucleus observes an 'average' of the electronic states of high-

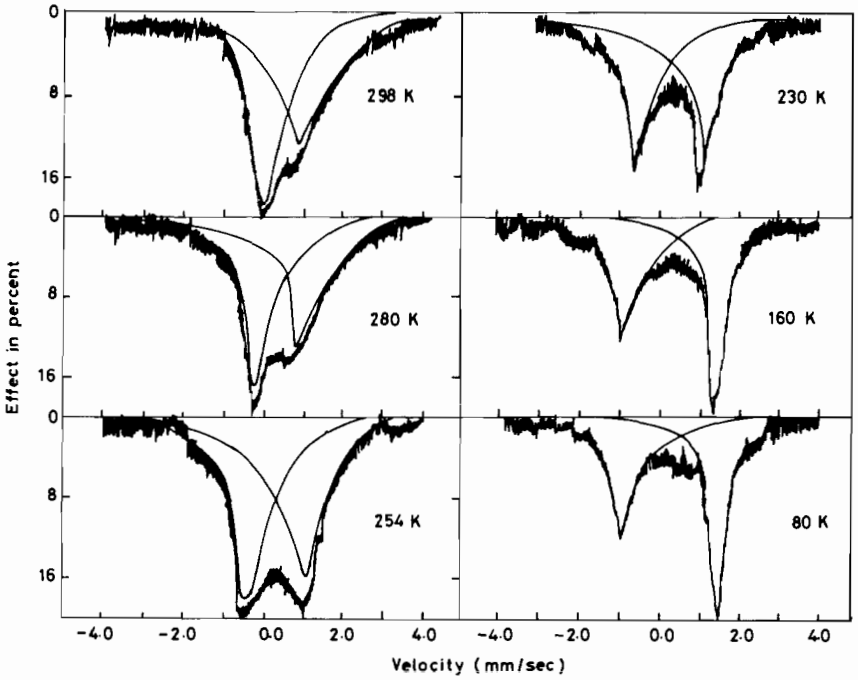

Fig. 5. Fe Mössbauer spectra of $[Fe(3\text{-}CH_3OSPH)_2]BPh_4$ at various temperatures.

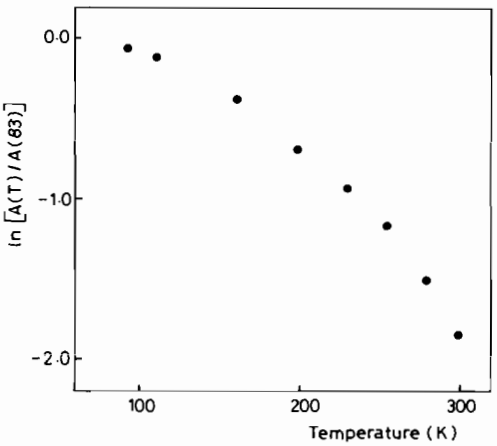

Fig. 6. Temperature dependence of the $\ln[A(T)/A(83)]$ parameters for $[Fe(3\text{-}CH_3OSPH)_2]BPh_4$.

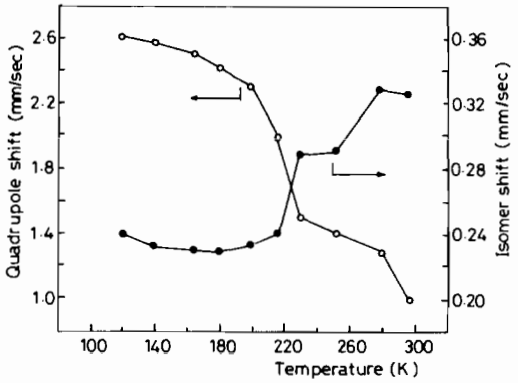

Fig. 7. Plot of Mössbauer quadrupole splitting (○) and isomer shift (●) *vs.* temperature for complex $[Fe(3\text{-}CH_3OSPH)_2]BPh_4$.

and low-spin states, *i.e.* the spin-state interconversion rates are more rapid than $\sim 10^7$ s^{-1}. The plot of $\ln[A(T)/A(83)]$ *versus* temperature for this complex is linear in the temperature range of spin transition, as illustrated in Fig. 6, suggesting that the spin interconversion observed in this complex is an intramolecular phenomenon [8, 11].

Figure 7 illustrates the variations of the δ and ΔE_Q values *versus* temperature. The drastic change in the δ values is characteristic of a high-spin iron(III) in the temperature range between 230–298 K and the values in the temperature range of a spin-crossover transition are intermediate between those of two spin-states and change with the population of high-(or low-) spin states. The large ΔE_Q values at low temperatures are characteristic of low-spin iron(III) complexes, resulting from a non-spherical electron distribution in the d orbitals. The ΔE_Q gradually approaches the limiting high-spin values with increase of temperature. The asymmetry of the quadrupole split doublet and the broadening of the lines in the Mössbauer spectra at high temperature is visually apparent. It has been shown that such broadening of the Mössbauer absorptions of any paramagnetic sample is possible when the spin–spin and/or spin–lattice relaxation times are of the same magnitude as the ^{57}Fe nuclear Larmor precessional frequency. As indicated by Blume [25], intermediate paramagnetic relaxation broadens the $|I = \frac{1}{2}, M_I = \pm\frac{1}{2}\rangle \rightarrow$

$|\frac{3}{2} \pm \frac{3}{2}\rangle$ quadrupole components more than it broadens the $|\frac{1}{2} \pm \frac{1}{2}\rangle \rightarrow |\frac{3}{2} \pm \frac{1}{2}\rangle$ component. At low temperature when the molecule is largely in the low-spin $S' = 0$ state, the negative-velocity quadrupole component is broader than the positive-velocity component for the iron(III) compound. From this it can be inferred that the principal-axis component of the electric field gradient (EFG) tensor, *Vzz*, is negative, a result consistent with the d_{xy} ground state, also indicated by EPR g tensor analyses.

It is evident from the Fig. 5 that the linewidth asymmetry at room temperature is opposite to that observed at low temperature. The high-spin asymmetry indicates a positive *Vzz*. It is not unreasonable that the signs of *Vzz* are opposite for the low- and high-spin electronic states of the same molecule. This observation is consistent with the data illustrated in Fig. 7. As discussed in theoretical terms by Maeda and Takashima [26] and in some detail by Hendrickson *et al.* [14], a minimum in the quadrupole splitting can be expected at some population ratio of high to low spin. Since the population ratio at which the minimum occurs is a sensitive fraction of the relative magnitudes of *Vzz* values, the relative orientations of the EFG tensors of high- and low-spin species, and the extent of deviation of each tensor from nonaxial symmetry, it is very likely that the curve (ΔE_Q *versus* temperature) illustrated in Fig. 7 corresponds to this predicted behaviour. The low-spin compounds $[Fe(3\text{-}CH_3OSPH)_2]Y$ ($Y = Cl^-$ or NO_3^-) exhibit a single quadrupole-split doublet in the ^{57}Fe Mössbauer spectra with a quadrupole splitting of $\Delta E_Q \simeq 2.75$ mm/s, in excellent agreement with the values reported for various analogues low-spin iron(III) complexes [22].

Electron Paramagnetic Resonance

In Figs. 8 and 9 are illustrated the X-band EPR spectra at various temperatures for $[Fe(3\text{-}CH_3OSPH)_2]PF_6$ and $[Fe(3\text{-}CH_3OSPH)_2]BPh_4$ compounds, respectively. At 298 K, the two EPR signals are observed, one at $g \simeq 4.2$ and the other at $g \simeq 2.0$. For the simple high-spin low-symmetry (rhombic) ferric complexes an intense signal near 4.3 is usually observed [27]. At low temperature, the EPR signal near 2.0 is well resolved, grows in intensity at the expense of the other signal $g \simeq 4.2$ as the temperature is lowered, and is characterized by rhombic symmetry in contrast with axial symmetry in a high-spin state. The difference of the molecular symmetry between the low- and high-spin states plays an important role in the spin-crossover mechanism. In addition, the observation of two distinct high- and low-spin resonances at each temperature indicates that the spin-state interconversion rates in the region of 78–300 K are considerably slower than the x-band frequency of $\sim 10^{10}$ s^{-1}.

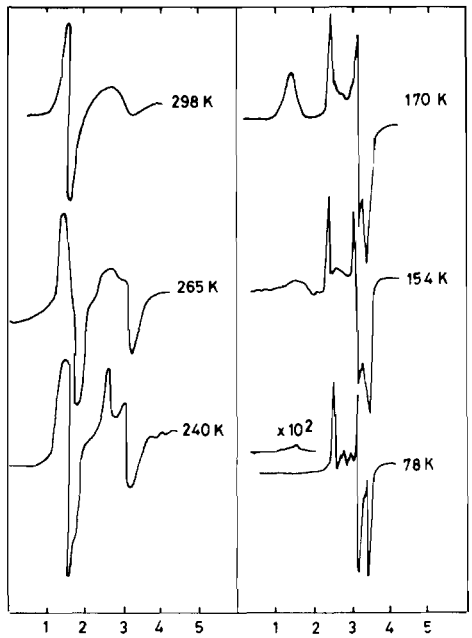

Fig. 8. X-band EPR spectra of $[Fe(3\text{-}CH_3OSPH)_2]PF_6$ at various temperatures.

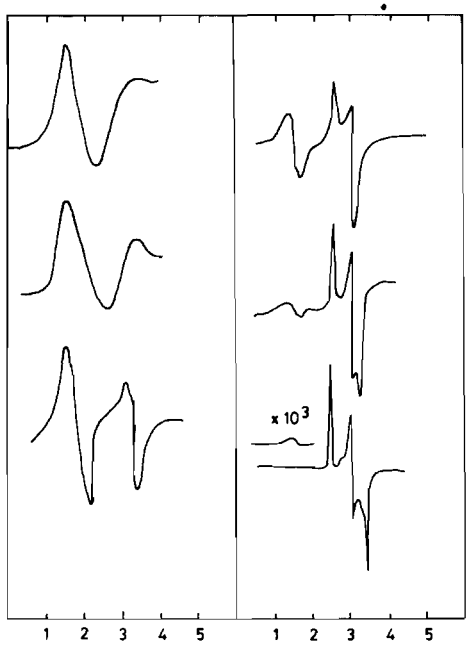

Fig. 9. X-band EPR spectra of $[Fe(3\text{-}CH_3OSPH)_2]BPh_4$ at various temperatures.

At low temperatures the EPR resonance observed at $g = 2.0$ for the ground-state Kramers doublet is well resolved. The g values for the two iron(III) complexes, listed in Table I, are used to determine the nature of the ground-state Kramers doublet. By the use of the Hamiltonian

TABLE I. Experimental and Calculated[a] EPR Parameters

Compound	g_x	g_y	g_z	A	B	C	E_1/λ	E_2/λ	E_3/λ
$[Fe(3\text{-}CH_3OSPH)_2]Cl$	−2.172	2.172	−1.982	−0.064	−0.998	0.000	−7.81	3.35	3.38
$[Fe(3\text{-}CH_3OSPH)_2]NO_3$	−2.134	2.134	−1.989	−0.052	−0.999	0.000	−9.37	4.17	4.21
$[Fe(3\text{-}CH_3OSPH)_2]PF_6$	−2.157	2.071	−1.987	−0.044	−0.999	+0.014	−12.70	−0.44	12.12
$[Fe(3\text{-}CH_3OSPH)_2]BPh_4$	−2.157	2.078	−1.988	−0.046	−0.999	+0.016	−12.07	−0.82	11.98

[a]Parameter definitions and methods of calculation are described in the text.

$$\mathcal{H} = -\lambda Is + (\mu/9)(3I_z^2 - I)(I+1) + (R/12)(I_+^2 + I_-^2)$$

acting upon the appropriate one-electron orbitals for the t_{2g} [5] configuration, three secular equations results for the Kramers doublet. In the Hamiltonian, λ is the spin–orbit coupling constant, μ is the axial ligand field distortion parameter, and R gauges the rhombic distortion. By considering the matrix elements of a Zeeman Hamiltonian, the secular equations can be solved to give wavefunctions [28]

$$g_z = -2[A^2 - B^2 + C^2 + k(A^2 - C^2)]$$

$$g_x = 2[2AC - B^2 + kB(2^{1/2})(C - A)]$$

$$g_y = -2[2AC + B^2 + kB(2^{1/2})(C + A)]$$

In the above expressions for the components of g tensor, k is the orbital reduction factor and the parameters A, B, and C are used to characterize the two spinors of the ground-state Kramers doublets [28].

$$\psi = A|+1^+\rangle + B(1/2)^{1/2}[|2^-\rangle - |-2^-\rangle] + C|-1^+\rangle$$

$$\psi = A|-1^-\rangle - B(1/2)^{1/2}[|2^+\rangle - |-2^+\rangle] + C|1^-\rangle$$

The values of A, B, and C were determined to solve the above three equations by using the experimental g values and are listed in Table I. In this calculation, the value of k is kept constant at 0.9. In addition, the energies of the three Kramers doublets of $^2T_{2g}$ origin (E_1/λ, E_2/λ, and E_3/λ) were obtained by solving the secular equations; these values are also listed in Table I. The large value of B (= 1.0) indicates that the unpaired electron in the ground Kramers doublet is in essentially a d_{xy} orbital and that the sign of the EFG is negative. Furthermore, if the value of λ is assumed to be 460 cm^{-1}, then the energy separation of the ground and first excited Kramers doublets is $\simeq$5000 cm^{-1}, a value much larger than thermal energies. This indicates that the low-spin magnetic moment and Mössbauer quadrupole splitting should be essentially temperature independent, and the temperature dependencies of these quantities can be attributed solely to spin-crossover origins. The experimental g values and calculated parameters for $[Fe(3\text{-}CH_3OSPH)_2]Y$ ($Y = Cl^-$ or NO_3^-) are also listed in Table I.

Spin-equilibrium Phenomena in Solution

The compound $[Fe(3\text{-}CH_3OSPH)_2]BPh_4$ is thermochromic in solution, changing from dark purple at room temperature to blue at 78 K in acetone. The colour change of the solution containing the compound is usually interpreted in terms of the change of the electronic ground state of the complex.

The variable temperature electronic spectrum of $[Fe(3\text{-}CH_3OSPH)_2]BPh_4$ in methanol is illustrated in Fig. 10. In general, the spectrum is characterized by a low-energy charge-transfer band at 670 nm (14925 cm^{-1}) which increases in intensity with decreasing temperature, and a higher-energy band at 550 nm (18 180 cm^{-1}) which decreases with decreasing temperature. On the basis of this temperature dependent spectrum pattern and magnetic susceptibility data (*vide supra*), the low-energy band is assigned to the $^2T_2$ ($S = 1/2$) state and the high-energy band to the $^6A_1$ ($S = 5/2$) spin state. The observation of the

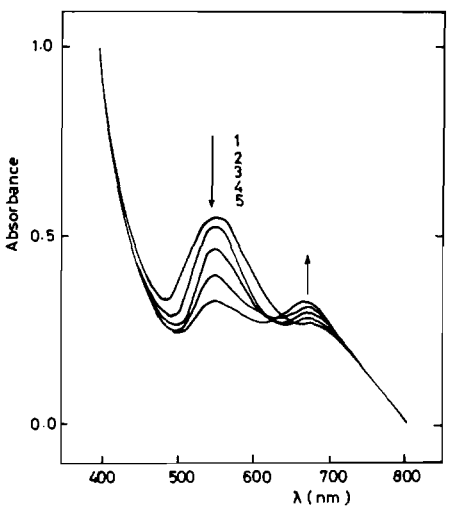

Fig. 10. Variable temperature electronic spectrum of $[Fe(3\text{-}CH_3OSPH)_2BPh_4$ in methanol at (1) 298 K, (2) 270 K, (3) 258 K, (4) 235 K and (5) 225 K.

separate low-spin and high-spin spectral bands indicates that the rate of the spin-interchange crossing process is slower than 10^{15} s^{-1} in solution. This result suggests that the rapid spin interconversion observed in the solid-state of the compound proceeds fundamentally through an intramolecular mechanism (electronic factor) and is also influenced by the combined electron–phonon excitation.

Acknowledgements

We thank Dr R. Bembi at the Department of Chemistry, Roorkee University, Roorkee, for use of the magnetometer. We also wish to thank Dr R. C. Sirivastava at the Department of Science and Technology, New Delhi for his interest in this work.

References

1 E. Konig, G. Ritter, W. Irler and H. A. Goodwin, *J. Am. Chem. Soc., 102,* 4681 (1980).
2 E. Konig, G. Ritter, S. K. Kulshreshtha and S. M. Nelson, *J. Am. Chem. Soc., 105,* 1924 (1983).
3 K. F. Purcell and M. P. Edwards, *Inorg. Chem., 23,* 2624 (1984).
4 P. Gutlich, *Struct. Bonding (Berlin), 44,* 83 (1981).
5 P. B. Merrithew and P. G. Rasmussen, *Inorg. Chem., 11,* 325 (1972).
6 K. R. Kunze, D. L. Perry and L. J. Wilson, *Inorg. Chem., 16,* 594 (1977).
7 D. DeFilipo, P. Depalano, A. Diaz, S. Steffe and F. E. Trogu, *J. Chem. Soc., Dalton Trans.,* 1566 (1977).
8 Y. Maeda, N. Tsutsumi and Y. Takashima, *Chem. Phys. Lett., 88,* 248 (1982).
9 Y. Maeda, H. Ohshio and Y. Takashima, *Chem. Lett.,* 943 (1982).
10 H. Ohshio, Y. Maeda and Y. Takashima, *Inorg. Chem., 22,* 2684 (1983).
11 Y. Maeda, N. Tsutsumi and Y. Takashima, *Inorg. Chem., 23,* 2440 (1984).
12 W. D. Federer and D. N. Hendrickson, *Inorg. Chem., 23,* 3861 (1984).
13 W. D. Federer and D. N. Hendrickson, *Inorg. Chem., 23,* 3870 (1984).
14 M. D. Timken, C. E. Strouse, S. M. Soltis, S. Daverio, D. N. Hendrickson, A. M. Abdel-Mawgoud and S. R. Wilson, *J. Am. Chem. Soc., 108,* 395 (1986).
15 M. D. Timken, A. M. Abdel-Mawgoud and D. N. Hendrickson, *Inorg. Chem., 25,* 160 (1986).
16 B. N. Figgis and J. Lewis, in J. Lewis and R. G. Wilkins (eds.), 'Modern Coordination Chemistry', Interscience, New York, 1960, p. 403.
17 A. P. Summerton, A. A. Diamantis and M. R. Snow, *Inorg. Chim. Acta, 27,* 123 (1978).
18 P. G. Sim, E. Sinn, R. H. Petty, C. L. Merrill and L. J. Wilson, *Inorg. Chem., 20,* 1213 (1981), and refs. therein.
19 M. D. Timken, D. N. Hendrickson and E. Sinn, *Inorg. Chem., 24,* 3947 (1985).
20 E. Sinn, P. G. Sim, E. V. Dose, M. F. Tweedle and L. J. Wilson, *J. Am. Chem. Soc., 100,* 3375 (1978).
21 P. A. Rock, 'Chemical Thermodynamics', MacMillan, London, 1969, pp. 188–9.
22 M. S. Haddad, M. W. Lynch, W. D. Federer and D. N. Hendrickson, *Inorg. Chem., 20,* 123 (1981).
23 R. H. Petty, E. V. Dose, M. F. Tweedle and L. J. Wilson, *Inorg. Chem., 17,* 1064 (1978).
24 R. H. Herber and Y. Maeda, *Physica B + C (Amsterdam), 99B,* 352 (1980).
25 M. Blume, *Phys. Rev. Lett., 14,* 96 (1965).
26 Y. Maeda and Y. Takashima, *Mem. Fac. Sci. Kyushu Univ. Ser. C, 14,* 107 (1983).
27 H. H. Wickman, M. P. Klein and D. A. Shirley, *J. Chem. Phys., 42,* 2113 (1965).
28 R. M. Golding, 'Applied Wave Mechanics', Van Nostrand, London, 1969.